Interaction of vortices with ultrasound and the acoustic Faraday effect in type-II superconductors

D. Domínguez* and L. Bulaevskii
Los Alamos National Laboratory, Los Alamos, New Mexico 87545

B. Ivlev†
Los Alamos National Laboratory, Los Alamos, New Mexico 87545
and Universidad Autónoma de San Luis Potosí, Instituto de Física, Álvaro Obregón 64, 78000 San Luis Potosí, San Luis Potosí, Mexico

M. Maley and A. R. Bishop
Los Alamos National Laboratory, Los Alamos, New Mexico 87545
(Received 31 May 1995; revised manuscript received 11 September 1995)

We study the interaction of sound waves with vortices in type-II superconductors, taking into account pinning and electrodynamic forces between vortices and crystal displacements. We propose ultrasound techniques as a method for obtaining information about vortex dynamics. This is particularly appropiate at low temperatures where transport measurements are ineffective. The changes in sound velocity and attenuation due to vortices, can provide information on the elastic constants of the vortex system and on vortex dissipation, respectively. At low temperatures the Magnus force acting on vortices leads to the *acoustic Faraday effect*: there is a rotation of the polarization plane of tranverse sound waves propagating along the magnetic field. This effect is linear in the Magnus force and magnetic field in crystals with equivalent a and b axes for a field parallel to the c axis. We discuss how this effect can be measured by means of either pulse-echo techniques or standing sound waves. Also, we show that an ac electromagnetic field acting on the vortex system can generate ultrasound. We calculate the amplitude of the generated sound waves in the linear regime and compare with recent experiments.

I. INTRODUCTION

In the presence of magnetic fields the transport and electromagnetic properties of superconductors are determined largely by the dynamical behavior of quantized vortices. Their motion when driven by currents produces dissipation which takes place predominantly in the normal core of vortices. Understanding the mechanisms that control vortex motion and dissipation is therefore important for applications of superconductors because they determine losses in the superconducting state.

When in motion, superconducting vortices are subject to several forces including Lorentz, viscous,[1] and hydrodynamic or Magnus[2] forces, resulting in components both parallel and normal to their instantaneous velocity. The resultant motion depends upon the relative magnitudes of these forces and is therefore field and temperature dependent. The complexity of this situation and the difficulty of separating the effects of the various components is responsible for the fact that phenomena such as the Hall effect in the mixed state, which depend upon the details of vortex motion, are still controversial after many years of study. This situation is further complicated for high-temperature superconductors by the small size of the normal core which results in discrete, well-separated states in the core, leading to the expectation that viscous dissipation may be ''frozen out'' at low temperature.[3] The low-temperature vortex dynamics depends strongly on the type (especially symmetry) of the superconducting pairing, so that obtaining information on vortex dynamics in this temperature region may also help to understand the pairing mechanism in high-T_c superconductors. Additionally, the low-temperature dynamics of vortices is of great interest for fundamental quantum-statistical physics because of the quantum effects on vortex motion: To a large degree it resembles the behavior of electons in a very strong magnetic field, where a quantum Hall effect has been studied recently.[4]

Until now the only information available on high-temperature vortex dynamics comes from transport measurements. Such methods are ineffective for providing information on the low-temperature behavior of vortices, because here strong pinning suppresses vortex transport. In fact, information on vortex dynamics available now from transport measurements covers the temperatures above 13 K for Y-Ba-Cu-O with $T_c = 60$ K (Ref. 5) and above 50 K in Bi-Sr-Ca-Cu-O.[6] A method to study vortex dynamics based on measurements of sound propagation in the vortex state of type-II superconductors was proposed by Pankert[7] and extended to the low-temperature regime by Domínguez *et al.*[8,9]

Pankert argued that the coupling of sound waves with vortices via pinning leads to a modified attenuation and dispersion of sound. The modification of the dispersion (sound velocity) comes from the involvement of vortices in crystal displacements and therefore there is an addition of vortex lattice elasticity to the crystal elasticity. The attenuation of sound was predicted by Pankert for the thermally activated flux flow (TAFF) regime valid above the irreversibility line: It originates from thermally activated jumps of vortices between pinning centers when vortices follow oscillating pinning centers. Experimental data[10] confirmed the main theoretical predictions of Pankert in that temperature range.

At low temperatures the Magnus force becomes important

for vortex dynamics and it results in novel effects: the change of sound polarization, as was discussed in Refs. 8,9. In the following we will present a detailed consideration of sound progation in the mixed state of type-II superconductors, taking into account all mechanisms of the sound-vortex interaction and all forces acting on vortices (Sec. II). Our main attention will be given to the effect of the Magnus force for vortices on the propagation of sound at low temperatures (Secs. III and IV, and the Appendix for a general approach). This results in a new effect: namely, the Faraday rotation of sound polarization. We will discuss possible experiments with ultrasound to extract the parameters of Magnus and viscous forces acting on vortices (Sec. V) and the generation of sound waves by an ac magnetic field acting on vortices (Sec. VI).

II. GENERAL EQUATIONS

We use the London model to describe vortices so that our approach is valid only well below T_c. The equation of motion for displacements of vortices from their equilibrium positions $\mathbf{v}(\mathbf{r},t)$ is

$$\eta_v\dot{\mathbf{v}}+\alpha_M[\dot{\mathbf{v}}\times\mathbf{n}]-(C_{11}-C_{66})\nabla_\perp \mathrm{div}(\mathbf{v})+C_{66}\nabla_\perp^2\mathbf{v}+\hat{C}_{44}\frac{\partial^2}{\partial^2 z}\mathbf{v}=-\frac{1}{c}[\mathbf{j}\times\mathbf{B}]+\alpha_p(\mathbf{u}_\perp-\mathbf{v}), \tag{1}$$

where we take $\mathbf{B}$ along the c (z) axis, $\mathbf{n}$ is the unit vector along $\mathbf{B}$, and $\mathbf{u}$ is the crystal displacement in the sound wave. The vortex displacements have only components in the x,y plane, $\mathbf{v}=(v_x,v_y)$, and thus the interaction is only with $\mathbf{u}_\perp=(u_x,u_y)$, and we have $\nabla_\perp=(\partial/\partial x,\partial/\partial y)$. The vortex inertial term is omitted here because it is small in comparison with the other dynamic terms on the left-hand side, as follows from estimates of vortex mass: See Refs. 11,12.

The theoretical prediction for the Magnus force coefficient made by Nozières and Vinen[2] by extension of ideal fluid results to superconductors is $\alpha_M=\pi\hbar n_s(B/\Phi_0)$, where n_s is the density of superconducting electrons. There are different contributions to α_M: Kopnin and Kravtsov[3] have shown that in s-wave BCS superconductors the contribution of quasiparticles inside the vortex core decreases this result at nonzero temperatures. They concluded that the Nozières–Vinen result remains valid in the limit $T\to 0$ in the superclean regime when the electron scattering rate becomes smaller than the separation of the energy levels of quasiparticles inside the normal core, $\approx\Delta^2/E_F$ (Δ is the superconducting gap). Another contribution to α_M is related to the dynamics of the order parameter, as shown by Kopnin *et al.*[13] and by Dorsey;[14] see also Ref. 15. Experimental measurements (see, for example, Ref. 16) show that at low temperatures α_M has the same sign as in the normal state and subsequently changes sign twice with increasing temperature in the temperature region below T_c. In high-T_c superconductors the sign of α_M is positive in the normal state due to the hole-type conductivity in these materials.

The estimate for η_v obtained by Bardeen and Stephen[1] and associated with dissipation caused by quasiparticles inside the vortex core is $\eta_v=BH_{c2}\sigma_n/c^2$, where σ_n is the conductivity in the normal state. In an s-wave superconductor in a superclean limit at low temperatures viscosity η_v tends to zero. In a gapless superconductor η_v remains finite in the limit $T\to 0$.[17]

C_{11}, C_{44}, and C_{66} are the compression, tilt, and shear modulii of the vortex system. For uniform distortions (i.e., long wavelengths) the elastic modulii can be obtained from thermodynamic arguments,[18]

$$C_{44}(0)=\frac{BB_a}{4\pi},$$

$$C_{11}(0)-C_{66}=\frac{B^2}{4\pi}\frac{dB_a}{dB}; \tag{2}$$

here $C_L(0)=C_{11}(0)-C_{66}$ is the modulus for isotropic compression, B_a is the applied field, and $B(B_a)$ defines the magnetization curve (for $B>2H_{c1}$, one has $B\approx B_a$). For deformations with wavelengths smaller than the London penetration length, the vortex system is softer than for homogeneous strains and the elasticity becomes nonlocal.[19] For a vortex lattice in an anisotropic superconductor, the nonlocal elastic modulii, for distortions with wave vector $\mathbf{k}$, are given by[19]

$$C_{44}(\mathbf{k})=\frac{B^2}{4\pi}\left[\frac{1}{1+\lambda_c^2(k_x^2+k_y^2)+\lambda_{ab}^2k_z^2}+\frac{\Phi_0 f(k_z)}{4\pi B\lambda_{ab}^2}\right], \tag{3}$$

$$C_{11}(\mathbf{k})=C_L(\mathbf{k})+C_{66}=\frac{B^2}{4\pi}\left[\frac{1+\lambda_c^2k^2}{(1+\lambda_{ab}^2k^2)(1+\lambda_c^2(k_x^2+k_y^2)+\lambda_{ab}^2k_z^2)}\right], \tag{4}$$

$$C_{66}=\frac{\Phi_0 B(1-B/H_{c2})^2}{(8\pi\lambda_{ab})^2}, \tag{5}$$

with $f(k_z)=1/2\gamma^2\ln[\xi_c^{-2}/(\lambda_{ab}^{-2}+k_z^2+4\pi\gamma^2\Phi_0/B)]+1/2k_z^2\lambda_{ab}^2\ln[1+k_z^2/(\lambda_{ab}^{-2}+4\pi\Phi_0/B)]$. Here λ_c is the penetration length for currents along the c axis, λ_{ab} is the penetration length for currents in the ab directions, and ξ_c and ξ_{ab} are the corresponding superconducting correlation lengths. For sound waves, k is small and the elastic modulii of the vortex lattice can be taken as $C_{11}=C_{44}=B^2/4\pi$ and $C_{66}=B\Phi_0/(8\pi\lambda_{ab})^2$ in superconductors with small and moderate anisotropy at high magnetic fields.[19] However, in Bi-2:2:1:2 the anisotropy ratio $\gamma=\lambda_c/\lambda_{ab}$ was estimated to be as large as 300–1000; see Ref. 20. For sound frequency 10 MHz and velocity $c_t=2\times10^5$ cm/s we obtain $k\lambda_c\approx1.7$ at $\gamma=300$ and $\lambda_{ab}=1700$ Å. In this case the dispersion of the tilt modulus (at high fields), $C_{44}(k)=B^2/4\pi[1+\lambda_c^2(k_x^2+k_y^2)+\lambda_{ab}^2k_z^2]$, becomes important. For a vortex liquid, the elastic modulii can be defined within a hydrodynamic approach in a coarse-grained free energy.[21] The tilt modulus of the liquid is identical to that of the vortex lattice as given by Eq. (3).[21] The liquid bulk modulus $C_L(\mathbf{k})$ can be obtained from the compressional modulus $C_{11}(\mathbf{k})$ of the lattice by setting $C_{66}=0$ in Eq. (4),[21] since the shear modulus is zero in the vortex liquid state. In the presence of strong pinning, i.e., for a vortex glass phase, the elastic constants are slightly renormalized by the disorder.[22–25] At very large length scales the compression and tilt modulus are still given by $C_{11}=C_{44}=B^2/4\pi$, as prescribed by the thermodynamic results of Eq. (2). It has been argued[26] that disorder can lead to the presence of dislocations in the lattice for scales $R>R_a$ [R_a defined as $\langle u^2(R_a)\rangle\approx a_0^2$, thus of the order of $R_a\approx(a_0/\xi)^2R_c$ with R_c the Larkin-Ovchinikov length[27] and $a_0=(\Phi_0/B)^{1/2}$ the intervortex distance]. Then the shear modulus may be renormalized as $C_{66}(k)\propto k^{2\beta}$ for $k\to0$ by the presence of dislocations,[25] so that the system may behave as a liquid at large length scales. (See the discussion in Sec. VII C of Ref. 25). Recently Giamarchi and Le Doussal[24] have shown that the elastic properties of the original vortex lattice are not destroyed by weak disorder, forming a so-called "Bragg glass" without dislocations (so the shear modulus is not driven to zero for $k\to0$ in this case). Here we will take C_{11},C_{44},C_{66} as parameters in Eq. (1), and we will show how their actual values for long wavelengths can be obtained from ultrasound measurements. Our phenomenological approach is valid for sound wavelengths that are much larger than the intervortex distance a_0, so that the vortex displacement field $\mathbf{v}(\mathbf{r})$ can be regarded as a continuous function of $\mathbf{r}$.

The first term in the right-hand side of Eq. (1) is the Lorentz force acting on the vortex due to the current $\mathbf{j}$ caused by ion motion. This force can be expressed through the lattice displacement $\mathbf{u}$ using the expression for the current density:

$$\mathbf{j}=\frac{c}{4\pi}[\nabla\times[\nabla\times\mathbf{A}]]=-\frac{c}{4\pi\lambda_{ab}^2}\mathbf{A}+en_I\dot{\mathbf{u}}. \tag{6}$$

The first term in the right-hand side is the electron current and the second one is the current of lattice ions;[28] n_I is the ion density. Such an expression for the total current implies the absence of impurities (weak momentum relaxation). In this case there is no drag of electrons by impurities. We also ignore the effect of electron drag by ions in a pure sample. This effect exists as soon as the electron spectrum in a crystal differs from the spectrum of a free electron. The electron drag by ions results in the renormalization of the ionic current in Eq. (6). Using (6) we can obtain $\mathbf{j}$ as a function of $\mathbf{u}$ and replace it in (1). Therefore we obtain the dynamical equation in Fourier space for $\mathbf{v}(\mathbf{k},\omega)$:

$$i\omega\left[\eta_v v_i+\epsilon_{ijz}\left(\alpha_M v_j+\alpha_I\frac{\lambda_{ab}^2k^2}{1+\lambda_{ab}^2k^2}u_j\right)\right]=[(C_{11}-C_{66})k_ik_j+C_{66}k_mk_m\delta_{ij}]v_j+C_{44}k_z^2v_i+\alpha_p(v_i-u_i), \tag{7}$$

where $i=x,y$ are coordinates in the ab plane, ϵ_{ijk} is the unit antisymmetric tensor, and ω is the frequency of sound. The term with coefficient $\alpha_I=\pi\hbar n_IB/\Phi_0$ takes into account the Lorentz force acting on vortices due to the current induced by moving ions and screened by superconducting electrons, and the sign of α_I is positive since it is determined by the ionic charge; λ_{ab} is the penetration length for currents along the layers.[28] This term is important only for frequencies $\omega/2\pi=c_sk/2\pi\geqslant1$ GHz and it will be omitted in the following. Here c_s is the sound velocity.

The term $\alpha_p(\mathbf{v}-\mathbf{u})$ was introduced by Pankert[7] to describe the interaction of sound waves with vortices because of pinning in the TAFF regime. In the absence of sound waves ($\mathbf{u}=0$) Eq. (7) with

$$\alpha_p=\alpha_L(1-i/\omega\tau_T)^{-1} \tag{8}$$

was used by many authors; see Refs. 29–31. Here α_L is the Labusch constant and τ_T is the relaxation rate which takes into account thermally activated hopping of vortices between different pinning centers. Using heuristic arguments, Brandt[29] obtained

$$\tau_T=(\eta_v/\alpha_L)\exp[U(B)/T], \tag{9}$$

where $U(B)$ is the characteristic pinning potential barrier. A similar expression was obtained by Coffey and Clem for a periodic pinning potential.[30] The generalization made by Pankert is transparent: Replacement of $\mathbf{v}$ by $(\mathbf{v}-\mathbf{u})$ accounts for the absence of pinning when vortices and ions move with the same velocity. We will use the same term $\alpha_p(\mathbf{v}-\mathbf{u})$ below the irreversibility line as well, thus neglecting jumps of vortices between pinning centers in the vortex glass phase.[26] This is valid for large frequencies such that $\omega\tau_T>1$,[31] meaning temperatures $T<U/\ln(\alpha_L/\omega\eta_v)$. For the typical ultrasound frequencies (10 MHz) and the parameters of the samples studies in, for example, Ref. 10, this is valid for $T<30$ K. When approaching the vortex glass transition this

approximation ceases to be valid. Here we will take this form of $\alpha_p(\omega,T)$ as a qualitative interpolation between the low-temperature regime of strong pinning where $\alpha_p \approx \alpha_L$ and the high-temperature (above the irreversibility line) TAFF regime where $\alpha_p \approx i\omega\tau_T\alpha_L$. The Labusch parameter may be expressed in terms of the critical current J_c as $\alpha_L = J_c B/cr_p$, where r_p is the pinning interaction range (approximately the superconducting coherence length ξ_{ab} in high-T_c superconductors).[31] For Bi-2:2:1:2 the critical current is in the range $(5\times10^5-5\times10^6)$ A/cm^2 at helium temperature in magnetic fields of several T (see Ref. 32), and we estimate $\alpha_L\Phi_0/B$ in the interval $(5\times10^4-5\times10^5)$ g/cm s^2. From the resistivity data[10] in this system in the TAFF regime, $U\approx 500$ K.

The equation for crystal displacements is

$$\rho\ddot{\mathbf{u}} + D\dot{\mathbf{u}} - (\lambda+\mu)\nabla \mathrm{div}(\mathbf{u}) - \mu\nabla^2\mathbf{u} = \mathbf{F}_i - \alpha_p(\mathbf{u}_\perp - \mathbf{v}), \quad (10)$$

where λ and μ are the elastic modulii of the crystal and ρ is the crystal mass density. (The u_z component is decoupled.) The term with the coefficient $D=\eta_0+\eta_q$ accounts for sound dissipation in the absence of vortices (η_0) and sound dissipation caused by quasiparticles inside the vortex core (η_q). The second term on the right-hand side of Eq. (10) is just opposite to the analogous term in Eq. (1). $\mathbf{F}_i$ is the force acting on ions from electrons. Within the same approximation as for Eq. (6) (ignoring electron drag), this force can be written as

$$\mathbf{F}_i = n_I\left(e\mathbf{E} + \frac{e}{c}[\dot{\mathbf{u}}\times\mathbf{B}]\right). \quad (11)$$

The electric field produced by vortices is $\mathbf{E}=[\mathbf{B}\times\dot{\mathbf{v}}]/c$ and the expression for $\mathbf{F}_i$ takes the form

$$\mathbf{F}_i = \frac{n_I}{c}[\mathbf{B}\times(\dot{\mathbf{v}}-\dot{\mathbf{u}})]. \quad (12)$$

Using Eq. (12), the equation for the crystal displacement in the Fourier components has the form

$$(\rho\omega^2 + i\omega D)u_i + i\omega\alpha_I\epsilon_{ijz}(u_j - v_j) = (\lambda+\mu)k_ik_ju_j + \mu k^2u_i + \alpha_p(u_i - v_i). \quad (13)$$

Besides pinning and electromagnetic forces, there is another mechanism for the vortex-sound interaction: Vortices induce strain in the superconducting crystal because they have normal cores where the specific volume is larger than in the superconducting state. This effect was discussed by Šimánek[12] in connection with the enhancement of the vortex mass. (The crystal displacements induced by moving a vortex have an additional kinetic energy.) The strain induced by vortices also provides an additional mechanism for the interaction of vortices, as discussed by Kogan *et al.*[33] The corresponding term in the equation of motion for crystal displacements u_i is $\eta_{\mathrm{str}}k_ik_j(u_j-v_j)$ and $\eta_{\mathrm{str}}\approx -2\xi_{ab}^2\lambda\zeta$. Here the superconducting correlation length inside the layers, ξ_{ab}, determines the area of the normal core. The coefficient ζ characterizes the relative change of specific volume in the normal and superconducting states, typically $\zeta\approx10^{-7}$–10^{-5}. Using these parameters and $\xi_{ab}\approx 20$ Å we estimate that the strain-induced vortex-sound interaction is negligible as compared with the pinning-induced interaction since $\eta_{\mathrm{str}}k^2/\alpha_L \sim 10^{-6}$ at least.

III. ULTRASOUND PROPAGATION PARALLEL TO THE MAGNETIC FIELD

Let us discuss first the case when the acoustic Faraday effect is maximum: sound propagation along the direction of the magnetic field $\mathbf{k}\|\mathbf{B}\|\mathbf{c}$ in crystals where a and b axes are equivalent (e.g., Bi- and Tl-based superconductors). We take $k_x=k_y=0$, $k_z=k$. We have from Eq. (7) for vortices

$$i\omega\eta_v v_x + i\omega\alpha_M v_y = C_{44}k^2v_x + \alpha_p(v_x-u_x),$$
$$i\omega\eta_v v_y - i\omega\alpha_M v_x = C_{44}k^2v_y + \alpha_p(v_y-u_y), \quad (14)$$

and from Eq. (13) for sound waves

$$(\rho\omega^2 + i\omega D)u_x + i\omega\alpha_I(u_y-v_y) = \mu k^2u_x + \alpha_p(u_x-v_x),$$
$$(\rho\omega^2 + i\omega D)u_y - i\omega\alpha_I(u_x-v_x) = \mu k^2u_y + \alpha_p(u_y-v_y),$$
$$(\rho\omega^2 + i\omega D)u_z = (\lambda+2\mu)k^2u_z, \quad (15)$$

for an isotropic material in the ab plane. In the absence of an interaction ($\alpha_p=\alpha_I=0$) the sound propagates either with transverse waves (u_x,u_y) with velocity $c_t=\sqrt{\mu/\rho}$, which are degenerate with respect to polarization, or with longitudinal waves (u_z) with velocity $c_l=\sqrt{(\lambda+2\mu)/\rho}$. The u_z component is always decoupled, and thus the longitudinal sound waves are unaffected by the presence of vortices.

We solve for $\mathbf{v}$ in (14) and substitute in (15), obtaining the effective equations for transverse sound waves (in first order in α_M,α_I):

$$[U-\alpha_p(1-g)]u_x + i\omega[\alpha_I(1-g)+\alpha_M g^2]u_y = 0, \quad (16)$$
$$-i\omega[\alpha_I(1-g)+\alpha_M g^2]u_x + [U-\alpha_p(1-g)]u_y = 0,$$

where $U=\rho\omega^2-\mu k^2+i\omega D$, $V=C_{44}k^2+\alpha_p-i\omega\eta_v$, with $g=\alpha_p/V$. The conditions $U=0$ and $V=0$ give the unperturbed dispersion relations for sound and vortices, respectively.

The modified dispersion relation can be obtained from solving

$$U-\alpha_p(1-g) = \pm\omega[\alpha_I(1-g)+\alpha_M g^2]. \quad (17)$$

The solution can be written in the general form

$$\rho\omega^2 - \rho\tilde{c}_t^2k^2 + i\omega\tilde{D} = \pm\omega(F+i\omega\Gamma), \quad (18)$$

where $\tilde{c}_t$ is the modified transverse sound velocity, $\tilde{D}$ is the modified dissipation coefficient, and F and Γ account for the circular polarization effect in sound velocity and dissipation (the latter effect is always negligible, $\omega\Gamma\ll\tilde{D}$; see the Appendix). From Eqs. (16), we can see that the eigenwaves satisfy

$$u_x/u_y = \pm i; \quad (19)$$

i.e., the sound is circularly polarized due to Magnus and electromagnetic forces. The split in sound velocity for different circular polarizations is $\tilde{c}_{t,\pm}=\tilde{c}_t(1\pm F/2\rho\omega)$. If ultra-

sound with a given polarization is introduced at one boundary of the sample, after traveling a length ℓ the polarization plane will rotate. This is the *acoustic Faraday effect*. The rotation angle per unit length will be given by $\theta/\ell=\omega/2(1/\tilde{c}_{t,-}-1/\tilde{c}_{t,+})\approx F/2\rho\tilde{c}_t$.

With the definitions $\mathcal{Q}=(C_{44}k^2+\alpha_T)^2+\omega^2(\eta_v+\eta_T)^2$, $\alpha_p=\alpha_T-i\omega\eta_T$, $\alpha_T=\alpha_L\omega^2\tau_T^2/(1+\omega^2\tau_T^2)$, and $\eta_T=\alpha_L\tau_T/(1+\omega^2\tau_T^2)$, the solution for the modified transverse sound velocity is

$$\tilde{c}_t^2=c_t^2+\frac{C_{44}}{\rho}\frac{\omega^2\eta_T^2+\alpha_T(C_{44}k^2+\alpha_T)}{\mathcal{Q}}+\frac{\alpha_T\omega^2\eta_v^2}{\rho k^2\mathcal{Q}}, \tag{20}$$

for the dissipation,

$$\tilde{D}=D+\frac{\eta_T C_{44}^2k^4+\eta_v[\alpha_T^2+\omega^2\eta_T(\eta_v+\eta_T)]}{\mathcal{Q}}, \tag{21}$$

and for the circular polarization coefficient,

$$\begin{aligned}F=\alpha_M\{&[\alpha_T(C_{44}k^2+\alpha_T)+\omega^2\eta_T(\eta_v+\eta_T)]^2\\&-\omega^2[\eta_T C_{44}k^2-\alpha_T\eta_v]^2\}\mathcal{Q}^{-2}\\&+\alpha_I[C_{44}k^2(C_{44}k^2+\alpha_T)+\omega^2\eta_v(\eta_v+\eta_T)]\mathcal{Q}^{-1}.\end{aligned} \tag{22}$$

Let us consider the low-temperature regime ($\omega\tau_T\gg1$, meaning $T<40$ K in $Bi_{1.6}Pb_{0.4}Sr_2Cu_3O_y$ studied in Ref. 7). In this case $\alpha_T\approx\alpha_L$ is the largest parameter, $\alpha_L\gg\omega\alpha_M,\omega\eta_v,C_{11}k^2,C_{66}k^2,C_{44}k^2$, and η_T is negligible. In this limit vortices are completely involved in sound oscillations, i.e., $v_i\approx u_i$. Then, the modified sound velocity is simply

$$\tilde{c}_t^2=c_t^2+C_{44}/\rho, \tag{23}$$

and the modified dissipation is

$$\tilde{D}=D+\eta_v. \tag{24}$$

Therefore, a measurement of the change in sound velocity and dissipation will give direct information on C_{44} and η_v at low temperatures. Particularly, measurements as a function of the ultrasound wave vector k will give information on the dispersion of $C_{44}(k)$, and thus on γ through Eq. (3). The Faraday effect is dominated by the Magnus force,

$$F\approx\alpha_M. \tag{25}$$

The rotation angle $\theta/\ell=\alpha_M/2\rho c_t$ is about 7°/cm for $\alpha_M\Phi_0/B=10^{-6}$ g/cm s, $\rho\approx5$–7 g/cm^3, and $B=5$ T. Therefore a measurement of θ can provide direct information on the Magnus force constant α_M below 40 K. The advantage here is that for sound propagation the effects of vortex dissipation η_v and Magnus force α_M are decoupled in contrast to their effect on resistivity and Hall angle; see Ref. 16.

Note that the Magnus force acts on vortices in the same way as a magnetic field acts on electrons: A vortex rotates around its equilibrium position when displaced from such position. It is this rotation that leads to the change in sound polarization due to the sound-vortex interaction; see Fig. 1. A similar phenomenon occurs in a ferromagnet, where a change of sound polarization results from the rotation of magnetization, which is coupled with sound waves by the magnetostriction effect.[34]

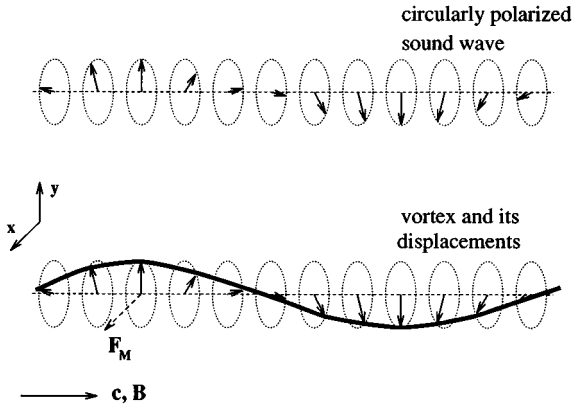

FIG. 1. Propogation of sound along the c axis of a unaxial crystal in the mixed state. The sound wave induces vortex displacements (shown below) due to pinning. They are circularly polarized because of the Magnus force $\mathbf{F}_M$. These circularly polarized displacements result in the rotation of sound polarization shown above.

Now we consider the high-temperature limit $\omega\tau_T\ll1$, where $\alpha_T\ll C_{44}k^2$ and $\eta_T\approx\eta_v\exp(U/T)$, so that $\alpha_p\approx-i\omega\eta_T$. In other words, at high temperatures the interaction through pinning mechanisms is via the TAFF viscosity η_T. In this limit $\tilde{c}_t$ in Eq. (20) reduces to the value calculated by Pankert,[7]

$$\tilde{c}_t^2=c_t^2+\frac{C_{44}}{\rho}\frac{\omega^2\eta_T^2}{C_{44}^2k^4+\omega^2\eta_T^2}, \tag{26}$$

the modified sound attenuation is

$$\tilde{D}=D+\eta_T\frac{C_{44}^2k^4}{C_{44}^2k^4+\omega^2\eta_T^2}+\eta_v\frac{\omega^2\eta_T^2}{C_{44}^2k^4+\omega^2\eta_T^2}, \tag{27}$$

which differs from that calculated by Pankert[7] in the η_v term, and the Faraday coefficient is

$$F=\alpha_M\frac{\omega^2\eta_T^2(\omega^2\eta_T^2-C_{44}^2k^4)}{(C_{44}^2k^4+\omega^2\eta_T^2)^2}+\alpha_I\frac{C_{44}^2k^4}{C_{44}^2k^4+\omega^2\eta_T^2}. \tag{28}$$

There is a peak for sound dissipation when $C_{44}k^2\approx\omega\eta_T$ (in Ref. 7 it occurs at about 60 K for $\omega/2\pi=3$MHz and $B=5$ T). Below the peak, $C_{44}k^2\ll\omega\eta_T$, and the circular polarization coefficient is given by $F\approx\alpha_M$. Above the peak, $C_{44}k^2\gg\omega\eta_T$, and we have $F\approx\alpha_I$. Therefore, at the dissipation peak there is a crossover in the Faraday effect from a regime dominated by the Magnus force to a regime dominated by the electrodynamic forces acting on the ions (α_I term) at high temperatures. This temperature behavior is schematically shown in Fig. 2.

IV. ULTRASOUND PROPAGATION PERPENDICULAR TO THE MAGNETIC FIELD

We now discuss the case of sound propagation perpendicular to the magnetic field, $\mathbf{k}\perp\mathbf{B}$, where we can take $k_y=k_z=0$, $k_x=k$.

We have for vortices

$$i\omega\eta_v v_x + i\omega\alpha_M v_y = C_{11}k^2 v_x + \alpha_p(v_x - u_x),$$

$$i\omega\eta_v v_y - i\omega\alpha_M v_x = C_{66}k^2 v_y + \alpha_p(v_y - u_y), \qquad (29)$$

and for sound waves

$$(\rho\omega^2 + i\omega D)u_x + i\omega\alpha_I(u_y - v_y) = (\lambda + 2\mu)k^2 u_x + \alpha_p(u_x - v_x),$$

$$(\rho\omega^2 + i\omega D)u_y - i\omega\alpha_I(u_x - v_x) = \mu k^2 u_y + \alpha_p(u_y - v_y), \qquad (30)$$

$$(\rho\omega^2 + i\omega D)u_z = \mu k^2 u_z,$$

for an isotropic material. Now, in the absence of interaction ($\alpha_p = \alpha_I = 0$) the sound propagation is transversal for the displacements u_y, u_z with velocity $c_t = \sqrt{\mu/\rho}$ and longitudinal for the displacements u_x with velocity $c_l = \sqrt{(\lambda + 2\mu)/\rho}$. In this case the u_z component of the transversal waves is always decoupled, whereas the other transversal component u_y and the longitudinal component u_x are coupled by the electromagnetic force.

Again, we solve for **v** in (29) and replace in (30) obtaining the effective equations for sound waves (in first order in α_M, α_I):

$$[U_1 - \alpha_p(1 - g_1)]u_x + i\omega[\alpha_I(1 - g_2) + \alpha_M g_1 g_2]u_y = 0,$$

$$-i\omega[\alpha_I(1 - g_1) + \alpha_M g_1 g_2]u_x + [U_2 - \alpha_p(1 - g_2)]u_y = 0, \qquad (31)$$

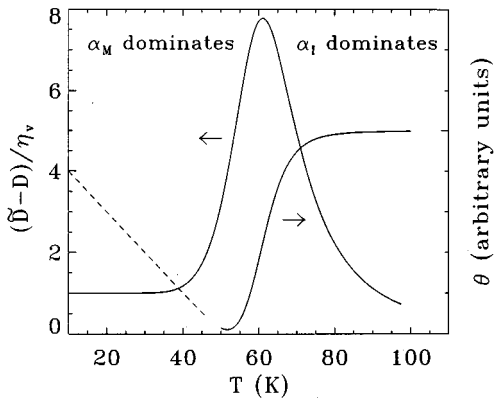

FIG. 2. The sound dissipation $\tilde{D}$-D due to vortex dynamics and the Faraday angle θ as a function of temperature, calculated using Eqs. (21), (22), with the experimental parameters of Ref. 7 for $B = 5$ T and $\omega/2\pi = 3$ MHz. Here we assume that α_M is linear in T (dashed line) and η_v is temperature independent. This is only intended to be a guide to the reader, in order to show that θ and $\tilde{D}$-D at low T will give direct information on $\alpha_M(T)$ and $\eta_v(T)$.

where $U_1 = \rho\omega^2 - (\lambda + 2\mu)k^2 + i\omega D$, $U_2 = \rho\omega^2 - \mu k^2 + i\omega D$, $g_i = \alpha_p/V_i$ with $V_1 = C_{11}k^2 + \alpha_p - i\omega\eta_v$ and $V_2 = C_{66}k^2 + \alpha_p - i\omega\eta_v$. This leads to the eigenvalue equation

$$[U_1 - \alpha_p(1 - g_1)][U_2 - \alpha_p(1 - g_2)] = \omega^2[\alpha_I(1 - g_1) + \alpha_M g_1 g_2][\alpha_I(1 - g_2) + \alpha_M g_1 g_2]. \qquad (32)$$

The longitudinal and transversal components u_x, u_y are coupled because of the Magnus and electrodynamics forces; their eigenwaves are

$$\frac{u_x}{u_y} = i\sqrt{\frac{\rho\omega^2 + i\omega D^v - \rho(c_t^v)^2k^2}{\rho\omega^2 + i\omega D^v - \rho(c_l^v)^2k^2}}. \qquad (33)$$

Thus the sound is elliptically polarized in this case. Here we defined $(c_t^v)^2 = c_t^2 + C_{66}/\rho$, $(c_l^v)^2 = c_l^2 + C_{11}/\rho$, and $D^v = D + \eta_v$.

Let us first discuss the low-temperature limit $\omega\tau_T \gg 1$. Proceeding as in the previous section, we obtain the dispersion relation

$$\rho\omega^2 + i\omega D^v = \frac{\rho[(c_l^v)^2 + (c_t^v)^2]k^2}{2} \pm \sqrt{\frac{\rho^2[(c_l^v)^2 - (c_t^v)^2]^2k^4}{4} + \alpha_M^2\omega^2}. \qquad (34)$$

Considering that $\rho[(c_l^v)^2 - (c_t^v)^2]k^2/2 \gg \omega\alpha_M$ we obtain that the longitudinal sound waves are now quasilongitudinal with velocity

$$\tilde{c}_l^2 = (c_l^v)^2\left\{1 + \frac{1}{2}\frac{\alpha_M^2(c_l^v)^2}{\rho^2\omega^2[(c_l^v)^2 - (c_t^v)^2]}\right\} \qquad (35)$$

and a small elliptical polarization given by

$$\frac{u_x}{u_y} = i\frac{\rho[(c_l^v)^2 - (c_t^v)^2]k^2}{\alpha_M\omega}. \qquad (36)$$

On the other hand, the transversal wave along the y direction now becomes quasitransversal with velocity

$$\tilde{c}_t^2 = (c_t^v)^2\left\{1 - \frac{1}{2}\frac{\alpha_M^2(c_t^v)^2}{\rho^2\omega^2[(c_l^v)^2 - (c_t^v)^2]}\right\} \qquad (37)$$

and a small elliptical polarization given by

$$\frac{u_x}{u_y} = i\frac{\alpha_M\omega}{\rho[(c_l^v)^2 - (c_t^v)^2]k^2}. \qquad (38)$$

Therefore, the effect of elliptical polarization due to the Magnus force at low temperatures is negligibly small in this

case, of order $(\alpha_M/\rho\omega)^2$. Neglecting this effect, the modified sound longitudinal velocity is simply $\tilde{c}_l^2 = c_l^2 + C_{11}/\rho$, the modified transversal velocity along the y direction is $\tilde{c}_t^2 = c_t^2 + C_{66}/\rho$, and the modified dissipation $\tilde{D} = D + \eta_v$. Thus, measurements of ultrasound propagation perpendicular to **B** can give infomation on C_{11} and C_{66}.

At high temperatures, $\omega\tau_T \ll 1$, the elliptical polarization effect is also negligible for similar reasons as before, now of the order of $(\alpha_I/\rho\omega)^2$. If we neglect this contribution, the modified sound velocities are given as in Eq. (26) after the replacement $c_t \to c_l$ and $C_{44} \to C_{11}$ for the longitudinal waves and after $C_{44} \to C_{66}$ for the transversal waves along y. Also the change in sound attenuation is given by Eq. (27) after the same replacements.

In general, the change in the ultrasound propagation for any arbitrary direction can also be calculated. We discuss this general case in the Appendix.

V. SOUND ECHO AND STANDING WAVE MEASUREMENTS

The change of sound polarization and dissipation can be measured for traveling waves. The polarization of transverse sound rotates by the angle $\theta = \alpha_M \ell / 2\rho c_t$ when it propagates along the path ℓ in the direction of the c axis in an uniaxial crystal and parallel to **B**. The length of propagation may be enhanced using the pulse-echo technique.[35] For such measurements it is important that the direction of rotation (clockwise or counterclockwise) depend only on the direction of magnetic field, and not on the direction of propagation. For transverse sound, when the magnetic field **B** is along the direction of propagation, which coincides with the c axis of the uniaxial crystal, we obtain the maximum effect for the rotation of the sound polarization (acoustic Faraday effect). In this case the amplitude f_n of the nth echo is

$$f_n = f_0 \left| \cos\left(\frac{\alpha_M L n}{\rho c_t} \right) \right| \exp\left(- \frac{2\tilde{D} L n}{\rho c_t} \right), \tag{39}$$

where L is the length of the sample and $\tilde{D} = D + \eta_v$. The cosine term is due to the rotation of the polarization angle. Here the effect will be notable at low temperatures in the superclean regime where $\eta_v \lesssim \alpha_M$ (see Ref. 5) and D is small enough [$D \propto \exp(-\Delta/kT)$ for s-wave superconductors]. In this case, due to Faraday rotation, the amplitude of the nth echo oscillates with n. The period of oscillations, $2\pi\rho c_t/\alpha_M L$, is about 15 for a sample with thickness $L = 0.1$ cm along the c axis. The decay of echo amplitude is determined by sound attenuation. Again, a similar effect was observed previously in ferromagnetic crystals because of the magnetostriction effect.[34] When the propagating sound is perpendicular to the magnetic field **B**, sound waves are longitudinal, the rotation of polarization is negligible, and the multiple echo amplitude f_n is given by (39) but without the cosine term and with c_t replaced by c_l.

For standing sound waves the Magnus force lifts the degeneracy of the resonance frequency with respect to polarization, with a splitting of $\Delta\omega = \alpha_M/\rho$ for transverse waves along the direction of **B**. This value is ≈ 0.01 MHz in a field of 5 T. It can be observed for small dissipation $(D + \eta_v)/\rho \ll \Delta\omega$.

VI. GENERATION OF ULTRASONIC WAVES BY ac MAGNETIC FIELDS

In a recent experiment, Haneda and Ishiguro observed generation of ultrasonic waves in the mixed state of high-T_c superconductors induced by the motion of vortices subjected to an ac magnetic field.[36] In a polycrystalline Y-Ba-Cu-O sample under a dc magnetic field, a pulse of an ac magnetic field was generated with a coil attached to one end of the sample; see Fig. 3. After the supply of the ac pulse, acoustic waves were detected by a quartz transducer attached at the other end of the sample. Also the echo of the acoustic signal was detected by the coil as an ac magnetic field induced by the returning acoustic wave. These effects arise because an ac electromagnetic field excites vortex oscillations, and the motion of vortices and sound waves are coupled through pinning mechanisms. Therefore, as pointed out by Haneda and Ishiguro, these measurements may provide means to study the pinning and dynamics of vortices. In Ref. 36 a semiquantitative theoretical discussion of the experimental results was given, in the framework of the nonlinear regime of vortex motion. A theoretical treatment of these effects in the linear regime was given in Ref. 9. Here we present the main points of this latter consideration and results.

The ac magnetic field produced by the coil induces vortex displacements. To find them we notice that vortex displacements produce an ac magnetic induction $B_{\mathrm{ac},z} = B\,\mathrm{div}(\mathbf{v})$ for $\mathbf{B} \| \hat{\mathbf{z}}$ and $\mathbf{B}_{\mathrm{ac}} = B\,\partial\mathbf{v}/\partial x$ for $\mathbf{B} \| \hat{\mathbf{x}}$. At the boundary we should have $B_{\mathrm{ac},z}(0,t) = h_{\mathrm{ac}}(t)$, where $h_{\mathrm{ac}}(t)$ is the ac magnetic field produced by the coil. Thus we obtain the boundary condition for $\mathbf{v}(\mathbf{r},t)$:

$$\frac{\partial v}{\partial x} = \frac{h_{\mathrm{ac}}(t)}{B}, \quad x = 0, \tag{40}$$

with $v = v_x$ for $\mathbf{B} \| \hat{\mathbf{z}}$ and $v = v_z$ for $\mathbf{B} \| \hat{\mathbf{x}}$. The propagation of vortex displacements is described by Eq. (7) which is valid at distances larger than λ_{ab} from the sample surface at $x = 0$. As we see from Eq. (7), the characteristic length of variation of **v** is the ac penetration depth $\lambda_{\mathrm{ac}} = (B^2/4\pi\alpha_p)^{1/2}$ which is larger than λ_{ab} at fields $B \gtrsim 1$ T; see Refs. 29,31. The vortex displacements induce sound waves as described by Eq. (13). Equation (13) for crystal displacements should be solved using the boundary condition

$$\frac{\partial \mathbf{u}}{\partial x} = 0, \quad x = 0, \tag{41}$$

for a free crystal surface (in the absence of external forces acting on the surface).

Therefore, using Eqs. (7) and (13), one can describe the following processes.

(1) Under the magnetic ac pulse, displacements of vortices are induced. At this stage the crystal displacements u are much smaller than v, and the solution of (7) with boundary condition (40) for a semi-infinite sample is direct; see the analysis of Brandt[29] and van der Beek *et al.*[31]

(2) Once the displacements v are found, we can solve Eq. (13) for u, with $\mathbf{v}(\mathbf{r},t)$ as a drive term and boundary condition (41), to obtain the amplitude of the induced sound pulse.

(3) This sound wave will propagate along the crystal; it will reach the other side of the sample where it can be detected by a quartz transducer, and where it will be reflected producing an echo propagating back to the originating side. This wave propagation was described with the modified sound equations (7) and (13) in Ref. 8.

(4) The returning sound echo induces displacements of vortices of magnitude v_e, which in turn cause an ac magnetic field that can be detected in the coil.

Let us discuss these processes in the low-temperature Campbell regime,[31] where we can take $\alpha_p = \alpha_L$. To describe the first process we can drop the Magnus and viscous force terms in (7) since $\alpha_L/\omega \gg \eta, \alpha_M$. Then, taking into account that here $u \ll v$, we have[29,31]

$$v(x,t) = \frac{B h_{\rm ac}(t)}{4\pi \lambda_{\rm ac} \alpha_L} \exp(-x/\lambda_{\rm ac}). \tag{42}$$

In a second step, we find the amplitude of the generated sound, solving Eq. (13), which reduces to the wave equation

$$\frac{\partial^2 u}{\partial t^2} - c_s^2 \frac{\partial^2 u}{\partial x^2} = \frac{\alpha_L}{\rho} v(x,t). \tag{43}$$

Here $c_s = c_t$ for a longitudinal mode (excited when $\mathbf{B} \perp \hat{\mathbf{x}}$) and $c_s = c_l$ for a transversal mode (excited when $\mathbf{B} \| \hat{\mathbf{x}}$); see Fig. 3. The solution of (43) is given by the sum of the propagating wave $f(x - c_s t)$ (solution of the homogeneous equation with $v = 0$), plus the solution $g(x,t)$ of the inhomogeneous wave equation. The latter is

$$g(x,t) = -\frac{B \lambda_{\rm ac}}{4\pi \rho c_s^2} h_{\rm ac}(t) \exp(-x/\lambda_{\rm ac}), \tag{44}$$

where we have taken into account that $\omega \ll c_s/\lambda_{\rm ac}$, which is fulfilled for the typical magnetic fields and frequencies in the experiments. From the boundary condition $\partial u/\partial x = \partial(f+g)/\partial x = 0$ at $x = 0$, we finally get for the propagating wave

$$f(x) = \frac{B}{4\pi \rho c_s} \int_{t_0}^{-x/c_s} h_{\rm ac}(t)\, dt, \tag{45}$$

with t_0 the starting time of the initial ac pulse. Now we verify that $u(x,t) \ll v(x,t)$ by noting that $u/v \approx \lambda_{\rm ac}^2/\alpha_L \rho c_s^2 = B^2/\rho c_s^2 \ll 4\pi$, for reasonable magnetic fields. This allowed us to neglect u in Eq. (7), when we obtained the induced $v(x,t)$ in Eq. (42), and also in Eq. (43).

We see in Eq. (45) that the amplitude of the sound pulse reaching the other side of the sample is

$$f_0 \approx \frac{B h_0}{\rho c_s \omega}, \tag{46}$$

where h_0 is the amplitude of the ac magnetic pulse. Note that the sound amplitude is proportional to B and h_0 and it does not depend on pinning in the Campbell regime. Now the multiple echo can be found as was described in Sec. V. Finally, when the nth sound echo returns to the originating side, it induces vortex displacements $v_e(x,t) \approx f_n(x + c_s t)$. This is because, in Eq. (7), α_L is the largest parameter at low temperatures; i.e., pinning centers almost completely involve vortices. The vortex displacements now induce an ac magnetic field with amplitude

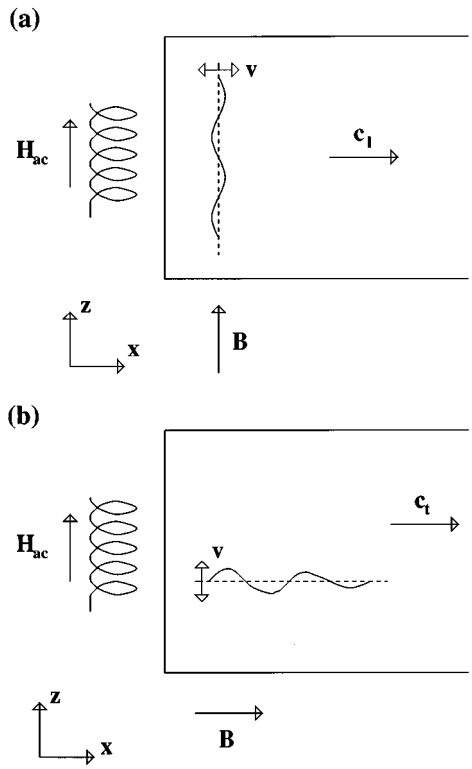

FIG. 3. Configurations of external magnetic field: (a) $\mathbf{B} \| \mathbf{H}_{\rm ac}$, generation of longitudinal sound waves propagating with velocity c_l; (b) $\mathbf{B} \perp \mathbf{H}_{\rm ac}$, generation of transversal sound waves propagating with velocity c_t. The direction of the induced displacements $\mathbf{v}$ in the vortex array is shown.

$$B_{\rm ac}^{(n)} = B \left| \frac{\partial v_e^{(n)}}{\partial x} \right| \approx \frac{h_0 B^2}{\rho c_s^2} \left| \cos\left(\frac{\alpha_M L n}{\rho c_s} \right) \right| \exp\left(-\frac{2\tilde{D} L n}{\rho c_s} \right). \tag{47}$$

The signal in the coil is proportional to $B_{\rm ac}^{(n)}$.

The condition for the linear regime is that the displacements of vortices at the surface (where they are maximum) are much smaller than the typical radius of the pinning centers. The latter is of the order of the correlation length ξ, and therefore we have the condition $|v(0,t)| \ll \xi$. We obtain for the amplitude of the electromagnetic pulse $h_0 \ll (4\pi J_c \xi B/c)^{1/2}$. For critical currents $J_c \approx 10^6$ A/cm this gives $h_0 \ll 50 (B/[1\ \mathrm{T}])^{1/2}$ G, which was obtained also in Ref. 32.

In the measurements of electromagnetic generation of ultrasound in Y-Ba-Cu-O by Haneda and Ishiguro,[36] an ac magnetic field with amplitude $h_0 = 50$ G was used at a temperature $T = 13$ K and dc magnetic fields up to 5 T. At $T = 13$ K these conditions correspond to the linear Campbell regime. The amplitude of the induced sound wave was found to be linear in B from 1 T up to 5 T, in agreement with our result of Eq. (46). The results of this section were recently confirmed in an experiment by Haneda, Ishiguro, and Murakami.[37]

VII. CONCLUSIONS

We have shown that the propagation of sound in the mixed state provides a powerful tool to investigate elasticity and dynamics of the vortex lattice, especially at low temperatures where transport measurements become ineffective for this purpose.

First, the rotation of sound polarization due to vortices gives information on the Magnus force. This acoustic Faraday effect is quite large in uniaxial superconductors when the magnetic field and the direction of sound propagation are along the c axis. In this geometry the linear Faraday effect may be observed. We note here that the acoustic Faraday effect can be obtained regardless of the question of whether the elastic properties are preserved in the vortex glass phase. The only requirement is that at low temperatures vortex lines move following the sound waves ($\mathbf{v}\approx\mathbf{u}$) due to strong pinning. This makes the Magnus force active on the sound displacements of transverse waves, inducing a rotation of the polarization plane. Also, the high frequency of the ultrasound oscillations makes negligible the effect of jumps between different metastable vortex glass configurations, which happen mainly at very large time scales. Therefore, the Magnus force coefficient can be extracted from the rotation of polarization for traveling waves and the change of polarization is approximately several degrees per cm in a field of 5 T at low temperatures. The path of sound propagation may be enlarged using the pulse-echo technique. This is possible only in the superclean limit, when the dissipation is smaller than the Magnus coefficient, $\eta_v<\alpha_M$. The same information may be extracted from splitting of standing wave resonances. Here the splitting is approximately 0.01 MHz in a field of 5 T at low temperatures. High-T_c Bi- and Tl-based uniaxial superconductors and low-T_c high-quality $NbSe_2$ crystals are good candidates for such study.

Second, the magnetic field dependence of sound velocity in the mixed state provides information on the elastic modulii of the vortex lattice. The most interesting case is the tilt modulus C_{44} which has a strong dispersion in highly anisotropic superconductors. It may be probed when sound propagates along the magnetic field direction and the c axis in uniaxial superconductors. Then measurements of field dependence of sound velocity provide quite direct information on the dispersion of C_{44} and thus on the anisotropy ratio γ. Information on this parameter obtained by other methods is not accurate until now.

Third, the field dependence of sound attenuation is determined by the contribution of quasiparticles inside the normal core and by the vortex viscosity. For superconductors with a gap the former is negligible, but in gapless superconductors both contributions may be important. Then attenuation of sound provides useful information on the symmetry and type of superconducting pairing.

ACKNOWLEDGMENTS

The authors thank A. Migliori for useful discussions. The work at Los Alamos National Laboratory is performed under the auspices of the U.S. DOE.

APPENDIX

For arbitrary directions of sound propagation and for crystals of any symmetry, we can study the dynamical equations for vortices and sound waves using tensor notation.

For vortices we have

$$[i\omega\eta_v\mathbf{I}+i\omega\alpha_M\mathbf{\Theta}_z-\mathbf{\Phi}(\mathbf{k})]\mathbf{v}=\alpha_p(\mathbf{v}-\mathbf{u}), \tag{A1}$$

where we have chosen z as the direction of the applied magnetic field, the elasticity tensor of the vortex lattice is $\Phi_{ij}(\mathbf{k})=(C_{11}-C_{66})k_ik_j+C_{66}k_\perp^2\delta_{ij}+C_{44}k_z^2\delta_{ij}$, $(\mathbf{\Theta}_z)_{ij}=\epsilon_{ijz}$ is the antisymmetric tensor, and $\mathbf{I}_{ij}=\delta_{ij}$ is the identity.

For sound waves the dynamical equations are

$$[\rho\omega^2\mathbf{I}-\mathbf{\Lambda}(\mathbf{k})+i\omega D\mathbf{I}]\mathbf{u}=[\alpha_p\mathbf{I}-i\omega\alpha_I\mathbf{\Theta}_z](\mathbf{u}-\mathbf{v}), \tag{A2}$$

where the elastic tensor is $\Lambda_{ij}(\mathbf{k})=\lambda_{im,lj}k_mk_l$ and for an isotropic material is $\lambda_{im,lj}=\lambda\delta_{im}\delta_{lj}+\mu(\delta_{il}\delta_{mj}+\delta_{ij}\delta_{ml})$.

Equations (48) and (49) can be reduced to an effective equation for sound waves of the form

$$[\rho\omega^2\mathbf{I}-\mathbf{\Lambda}_{\rm eff}(\mathbf{k})+i\omega\mathbf{D}_{\rm eff}(\mathbf{k})]\mathbf{u}=0\,, \tag{A3}$$

where $\mathbf{\Lambda}_{\rm eff}$ and $\mathbf{D}_{\rm eff}$ are Hermitian. We obtain

$$\begin{aligned}
\mathbf{\Lambda}_{\rm eff}=&\mathbf{\Lambda}+\alpha_T\mathbf{I}-i\omega\alpha_I\mathbf{\Theta}_z-(\alpha_T^2-\omega^2\eta_T^2)\left(\frac{\mathbf{G}+\mathbf{G}^*}{2}\right)+i2\omega\eta_T\alpha_T\left(\frac{\mathbf{G}-\mathbf{G}^*}{2}\right)\\
&+i\omega\alpha_I\alpha_T\left(\frac{\mathbf{\Theta}_z\mathbf{G}+\mathbf{G}^*\mathbf{\Theta}_z}{2}\right)+\omega^2\eta_T\alpha_I\left(\frac{\mathbf{\Theta}_z\mathbf{G}-\mathbf{G}^*\mathbf{\Theta}_z}{2}\right),\\
\mathbf{D}_{\rm eff}=&D\mathbf{I}+\eta_T\mathbf{I}-2\eta_T\alpha_T\left(\frac{\mathbf{G}+\mathbf{G}^*}{2}\right)-i\left(\frac{\alpha_T^2}{\omega}-\omega\eta_T^2\right)\left(\frac{\mathbf{G}-\mathbf{G}^*}{2}\right)\\
&-\alpha_I\alpha_T\left(\frac{\mathbf{\Theta}_z\mathbf{G}-\mathbf{G}^*\mathbf{\Theta}_z}{2}\right)+i\omega\alpha_I\eta_T\left(\frac{\mathbf{\Theta}_z\mathbf{G}+\mathbf{G}^*\mathbf{\Theta}_z}{2}\right),
\end{aligned} \tag{A4}$$

where we have taken $\alpha_p=\alpha_T-i\omega\eta_T$ and the vortex Green's function is defined as $\mathbf{G}=[\mathbf{\Phi}+\alpha_T\mathbf{I}-i\omega\alpha_M\mathbf{\Theta}_z-i\omega(\eta_v+\eta_T)\mathbf{I}]^{-1}$, which satisfies $\mathbf{G}^\dagger=\mathbf{G}^*$.

We can write $\mathbf{\Lambda}_{\rm eff}=\tilde{\Lambda}-i\omega\mathbf{F}$ with $\tilde{\Lambda}$ a real symmetric matrix and $\mathbf{F}$ a real antisymmetric matrix that breaks time-reversal symmetry and originates the rotation effect. Also for the generalized dissipation tensor we write $\mathbf{D}_{\rm eff}=\tilde{\mathbf{D}}-i\omega\mathbf{\Gamma}$ with $\tilde{\mathbf{D}}$ real

symmetric and $\mathbf{\Gamma}$ real antisymmetric. For α_M small we have $\mathbf{G}\approx\mathbf{G}_0+i\omega\alpha_M\mathbf{G}_0\mathbf{\Theta}_z\mathbf{G}_0$, with $\mathbf{G}_0=[\mathbf{\Phi}+\alpha_T\mathbf{I}-i\omega(\eta_v+\eta_T)\mathbf{I}]^{-1}$. Neglecting terms proportional to $\alpha_M\alpha_I$ we obtain

$$\tilde{\Lambda}=\mathbf{\Lambda}+\alpha_T\mathbf{I}-(\alpha_T^2-\omega^2\eta_T^2)\left(\frac{\mathbf{G}_0+\mathbf{G}_0^*}{2}\right)+i2\omega\eta_T\alpha_T\left(\frac{\mathbf{G}_0-\mathbf{G}_0^*}{2}\right),$$

$$\mathbf{F}=\alpha_M\left[(\alpha_T^2-\omega^2\eta_T^2)\left(\frac{\mathbf{G}_0\mathbf{\Theta}_z\mathbf{G}_0+\mathbf{G}_0^*\mathbf{\Theta}_z\mathbf{G}_0^*}{2}\right)-i2\omega\eta_T\alpha_T\left(\frac{\mathbf{G}_0\mathbf{\Theta}_z\mathbf{G}_0-\mathbf{G}_0^*\mathbf{\Theta}_z\mathbf{G}_0^*}{2}\right)\right]$$

$$+\alpha_I\left[\mathbf{\Theta}_z-\alpha_T\left(\frac{\mathbf{\Theta}_z\mathbf{G}_0+\mathbf{G}_0^*\mathbf{\Theta}_z}{2}\right)+i\omega\eta_T\left(\frac{\mathbf{\Theta}_z\mathbf{G}_0-\mathbf{G}_0^*\mathbf{\Theta}_z}{2}\right)\right],$$

$$\tilde{\mathbf{D}}=D\mathbf{I}+\eta_T\mathbf{I}-2\eta_T\alpha_T\left(\frac{\mathbf{G}_0+\mathbf{G}_0^*}{2}\right)-i\left(\frac{\alpha_T^2}{\omega}-\omega\eta_T^2\right)\left(\frac{\mathbf{G}_0-\mathbf{G}_0^*}{2}\right), \tag{A5}$$

$$\mathbf{\Gamma}=\alpha_M\left[2\alpha_T\eta_T\left(\frac{\mathbf{G}_0\mathbf{\Theta}_z\mathbf{G}_0+\mathbf{G}_0^*\mathbf{\Theta}_z\mathbf{G}_0^*}{2}\right)+i\left(\frac{\alpha_T^2}{\omega}-\omega\eta_T^2\right)\left(\frac{\mathbf{G}_0\mathbf{\Theta}_z\mathbf{G}_0-\mathbf{G}_0^*\mathbf{\Theta}_z\mathbf{G}_0^*}{2}\right)\right]$$

$$-\alpha_I\left[\eta_T\left(\frac{\mathbf{\Theta}_z\mathbf{G}_0+\mathbf{G}_0^*\mathbf{\Theta}_z}{2}\right)+i\frac{\alpha_T}{\omega}\left(\frac{\mathbf{\Theta}_z\mathbf{G}_0-\mathbf{G}_0^*\mathbf{\Theta}_z}{2}\right)\right].$$

In the low-temperature limit $\omega\tau_T\gg1$ we take $\mathbf{G}_0=1/\alpha_T\mathbf{I}-\mathbf{\Phi}/\alpha_T^2+i\omega(\eta_v+\eta_T)/\alpha_T^2\mathbf{I}$. We obtain

$$\tilde{\Lambda}=\mathbf{\Lambda}+\mathbf{\Phi}+\mathcal{O}\left(\frac{\omega^2\eta_T^2}{\alpha_T}\right),$$

$$\mathbf{F}=\alpha_M\mathbf{\Theta}_z+\mathcal{O}\left(\frac{\alpha_I\|\mathbf{\Phi}\|}{\alpha_T}\right),$$

$$\tilde{\mathbf{D}}=D\mathbf{I}+\eta_v\mathbf{I}+\mathcal{O}\left(\frac{\eta_T\|\mathbf{\Phi}\|}{\alpha_T}\right),$$

$$\mathbf{\Gamma}\approx\mathcal{O}\left(\frac{\alpha_I\eta_v}{\alpha_T}\right). \tag{A6}$$

In the high-temperature limit $\omega\tau_T\ll1$, taking into account that we can write $\mathbf{G}_0=[\mathbf{\Phi}+i\omega(\eta_v+\eta_T)\mathbf{I}][\mathbf{\Phi}^2+\omega^2\eta_T^2\mathbf{I}]^{-1}+\mathcal{O}(\alpha_T/\omega^2\eta_T^2)$, we obtain

$$\tilde{\Lambda}=\mathbf{\Lambda}+\mathbf{\Phi}\omega^2\eta_T^2(\mathbf{\Phi}^2+\omega^2\eta_T^2\mathbf{I})^{-1}+\mathcal{O}(\alpha_T),$$

$$\mathbf{F}=\alpha_M[\omega^2\eta_T^2(\omega^2\eta_T^2\mathbf{I}-\mathbf{\Phi}^2)(\mathbf{\Phi}^2+\omega^2\eta_T^2\mathbf{I})^{-1}\mathbf{\Theta}_z(\mathbf{\Phi}^2+\omega^2\eta_T^2\mathbf{I})^{-1}]+\alpha_I[\mathbf{\Theta}_z\mathbf{\Phi}^2(\mathbf{\Phi}^2+\omega^2\eta_T^2\mathbf{I})^{-1}]+\mathcal{O}\left(\frac{\alpha_I\alpha_T}{\omega\eta_T}\right),$$

$$\tilde{\mathbf{D}}=\mathbf{I}+\eta_T\mathbf{\Phi}^2(\mathbf{\Phi}^2+\omega^2\eta_T^2\mathbf{I})^{-1}+\eta_v\omega^2\eta_T^2(\mathbf{\Phi}^2+\omega^2\eta_T^2\mathbf{I})^{-1}+\mathcal{O}\left(\frac{\alpha_T}{\omega}\right), \tag{A7}$$

$$\mathbf{\Gamma}=2\alpha_M\omega^2\eta_T^3\mathbf{\Phi}(\mathbf{\Phi}^2+\omega^2\eta_T^2\mathbf{I})^{-1}\mathbf{\Theta}_z(\mathbf{\Phi}^2+\omega^2\eta_T^2\mathbf{I})^{-1}-\alpha_I\eta_T\mathbf{\Phi}(\mathbf{\Phi}^2+\omega^2\eta_T^2\mathbf{I})^{-1}\mathbf{\Theta}_z+\mathcal{O}\left(\frac{\alpha_I\alpha_T}{\omega^2\eta_T}\right).$$

Again, one can analyze the regimes below the dissipation peak, $\|\mathbf{\Phi}\|\ll\omega\eta_T$, and above the peak, $\|\mathbf{\Phi}\|\gg\omega\eta_T$, obtaining similar results as in the main body of the text (see Secs. III and IV). The term $\mathbf{\Gamma}$, not discussed before, is negligibly small: Below the peak it is $\omega\mathbf{\Gamma}\approx\mathcal{O}(\alpha_M\|\mathbf{\Phi}\|/\omega\eta_T)$, and above the peak it is $\omega\mathbf{\Gamma}\approx\mathcal{O}(\alpha_I\omega\eta_T/\|\mathbf{\Phi}\|)$. It only becomes relevant right at the dissipation peak, where the $\mathbf{F}$ term is negligibly small.

---

*Present address: Centro Atomico Barilioche, 8400 S. C. de Bariloche, Rio Negro, Argentina.

†On leave from Landau Institute for Theoretical Physics, Kosygin St. 2, Moscow, Russia.

[1] J. Bardeen and M.J. Stephen, Phys. Rev. **140**, A1197 (1965); M. Tinkham, Phys. Rev. Lett. **13**, 804 (1964).

[2] P. Nozières and W.F. Vinen, Philos. Mag. **14**, 667 (1966).

[3] N.B. Kopnin and V.E. Kravtsov, Pis'ma Zh. Eksp. Teor. Fiz. **23**,

631 (1976) [JETP Lett. **23**, 578 (1976)]; Zh. Eksp. Teor. Fiz. **71**, 1644 (1976) [Sov. Phys. JETP **44**, 861 (1976)].

[4] P. Ao and D.J. Thouless, Phys. Rev. Lett. **70**, 2158 (1993); L. Bulaevskii, A.I. Larkin, M. Maley, and V.M. Vinokur, Phys. Rev. B **52**, 9205 (1995); E.M. Chudnovsky and A. Vilenkin, J. Phys. Condens. Matter **7**, 6501 (1995).

[5] M. Harris, Y.F. Yan, O.K.C. Tsui, Y. Matsuda, and N.P. Ong, Phys. Rev. Lett. **73**, 1711 (1994).

[6] A.V. Samoilov, Z.G. Ivanov, and L.-G. Johansson, Phys. Rev. B **49**, 3667 (1994).

[7] J. Pankert, Physica B **165-166**, 1273 (1990); Physica C **168**, 335 (1990).

[8] D. Domínguez, L. Bulaevskii, B. Ivlev, M. Maley, and A.R. Bishop, Phys. Rev. Lett. **74**, 2579 (1995).

[9] D. Domínguez, L. Bulaevskii, B. Ivlev, M. Maley, and A.R. Bishop, Phys. Rev. B **51**, 15 649 (1995).

[10] J. Pankert *et al.*, Phys. Rev. Lett. **65**, 3052 (1990); M. Saint-Paul *et al.*, Physica C **180**, 394 (1991); M. Yoshizawa *et al.*, Solid State Commun. **89**, 701 (1994).

[11] H. Suhl, Phys. Rev. Lett. **14**, 226 (1965); M. Yu. Kupriyaniv and K. Likharev, Zh. Éksp. Teor. Fiz. **68**, 1506 [Sov. Phys. JETP **41**, 755 (1975)]; G. Blatter and V.B. Geshkenbein, Phys. Rev. B **47**, 2725 (1993).

[12] E. Šimánek, Phys. Lett. A **154**, 309 (1991).

[13] N.B. Kopnin, B.I. Ivlev, and V.A. Kalatsky, Pis'ma Zh. Eksp. Teor. Fiz. **55**, 717 (1992) [JETP Lett. **55**, 750 (1992)]; J. Low Temp. Phys. **90**, 1 (1993).

[14] A.T. Dorsey, Phys. Rev. B **46**, 8376 (1992).

[15] M.V. Feigel'man, V.B. Geshkenbein, A.I. Larkin, and V.M. Vinokur (unpublished).

[16] J.M. Harris, N.P. Ong, and Y.F. Yan, Phys. Rev. Lett. **71**, 1455 (1993); M.N. Kunchur, D.K. Christen, C.E. Klabunde, and J.M. Phillips, *ibid.* **72**, 2259 (1994).

[17] G.E. Volovik, Pis'ma Zh. Eksp. Teor. Fiz. **58**, 457 (1993) [JETP Lett. **58**, 468 (1993)].

[18] R. Labusch, Phys. Status Solidi **32**, 439 (1969); E. H. Brandt, Phys. Rev. B **34**, 6514 (1986).

[19] E.H. Brandt, J. Low Temp. Phys. **26**, 709 (1977); **28**, 291 (1977); A. Houghton, R.A. Pelkovits, and A. Sudbo, Phys. Rev. B **40**, 6763 (1989); L.I. Glazman and A.E. Koshelev, *ibid.* **43**, 2835 (1991); Physica C **173**, 180 (1991); E. H. Brandt, Rep. Prog. Phys. (to be published).

[20] R. Kleiner and P. Müller, Phys. Rev. B **49**, 1327 (1994); J.H. Cho *et al.*, *ibid.* **50**, 6493 (1994); A. Schilling *et al.*, Phys. Rev. Lett. **71**, 1899 (1993); Y. Iye *et al.*, Physica C **199**, 154 (1992); J.C. Martinez *et al.*, Phys. Rev. Lett. **69**, 2276 (1992).

[21] M.C. Marchetti, Phys. Rev. B **43**, 8012 (1991); M.C. Marchetti and D.R. Nelson, Physica C **174**, 40 (1991).

[22] Y.J.M. Brechet, B. Douçot, H.J. Jensen, and A.-Ch. Shi, Phys. Rev. B **42**, 2116 (1990); J. Ni and B. Gu, *ibid.* **49**, 15 276 (1994).

[23] J. P. Bouchaud, M. Mézard, and J. S. Yedidia, Phys. Rev. Lett. **67**, 3840 (1991).

[24] T. Giamarchi and P. Le Doussal, Phys. Rev. Lett. **72**, 1530 (1994); Phys. Rev. B **52**, 1242 (1995).

[25] G. Blatter, M.V. Feigel'man, V.B. Geshkenbein, A.I. Larkin, and V.M. Vinokur, Rev. Mod. Phys. **66**, 1125 (1994).

[26] D.S. Fisher, M.P.A. Fisher, and D.A. Huse, Phys. Rev. B **43**, 130 (1991).

[27] A.I. Larkin and Yu. N. Ovchinikov, J. Low Temp. Phys. **34**, 409 (1979).

[28] D.P. Belozorov and E. Kaner, Zh. Eksp. Teor. Fiz. **55**, 642 (1968) [Sov. Phys. JETP **28**, 334 (1969)]; I.E. Bulyzhenkov and B.I. Ivlev, *ibid.* **71**, 1172 (1976) [*ibid.* **44**, 613 (1976)]; G. Blatter and B. Ivlev, Phys. Rev. B **52**, 4588 (1995).

[29] E. H. Brandt, Phys. Rev. Lett. **67**, 2219 (1991).

[30] M.W. Coffey and J.R. Clem, Phys. Rev. Lett. **67**, 386 (1991); Phys. Rev. B **45**, 9872 (1992). Similar results were also obtained in P. Martinoli *et al.*, Physica (Amsterdam) **165-166B**, 1163 (1990).

[31] C.J. van der Beek, V.B. Geshkenbein, and V.M. Vinokur, Phys. Rev. B **48**, 3393 (1993).

[32] C.J. van der Beek, P.H. Kes, M.P. Maley, M.J.V. Menken, and A.A. Menovsky, Physica C **192**, 307 (1992); C.J. van der Beek and P. Kes, Phys. Rev. B **43**, 13 032 (1991).

[33] V.G. Kogan, L.N. Bulaevskii, P. Miranović, and L. Dobrosavljević-Grujić, Phys. Rev. B **51**, 15 649 (1995).

[34] H. Matthews and R. C. LeCraw, Phys. Rev. Lett. **8**, 397 (1962).

[35] R. Truell, C. Elbaum, and B.B. Chick, *Ultrasound Methods in Solid State Physics* (Academic, New York, 1969), p. 53.

[36] H. Haneda and T. Ishiguro, Physica C **235-240**, 2076 (1994).

[37] H. Haneda, T. Ishiguro, and M. Murakami, Physica B (to be published).